生物化学与生物物理学报
ISSN 0582-9879 ACTA BIOCHIMICA et BIOPHYSICA SINICA 2002, 34(3): 266 – 272 CN 31-1300/Q

Structure of an Acidic Phospholipase A_2 from the Venom of *Deinagkistrodon acutus* in a New Crystal Form

GU Li-Chuan, ZHANG Hai-Long, SONG Shi-Ying, ZHOU Yuan-Cong[1], LIN Zheng-Jiong *
(*National Laboratory of Biomacromolecules, Institute of Biophysics, the Chinese Academy of Sciences, Beijing* 100101, *China*;
[1] *Institute of Biochemistry and Cell Biology, the Chinese Academy of Sciences, Shanghai* 200031, *China*)

Abstract The three-dimensional structure of an acidic phospholipase A_2 purified from the venom of *Deinagkistrodon acutus* (*Agkistrodon acutus*) was determined in a new crystal form by molecular replacement at 0.28 nm resolution with a crystallographic *R* factor of 21.9% (*R*-free = 25.7%) and reasonable stereochemistry. Being similar to the previous reported crystal form, a significant conformational adaptation of segment 14—23 at the dimer interface was observed. This segment was related to the "interface recognition site" (IRS). It was found that a positively charged residue at position 34 seems to be a common feature for most of hemolytic PLA_2s belonging to group II. Structural comparison between the two crystal forms showed that NaCl had significant effects on the crystal packing, thus leading to dramatic changes of the unit cell parameters. In the new crystal form, MPD (2-methyl-2, 4-pentanediol) molecules exist in the hydrophobic channel of the enzyme.

Key words phospholipase A_2; X-ray crystallography; three-dimensional structure; hemolysis; interfacial catalysis

Phospholipase A_2 (PLA_2s, EC 3.1.1.4) catalyzes the hydrolysis of the fatty acid ester at the *sn*-2 position of phospholipids in a calcium-dependent reaction. The low molecular mass PLA_2s are classified into two main groups based on sequence and structural homology. It is well known that in addition to being a catalyst for the hydrolysis of phospholipids, PLA_2 from snake venom possesses a wide variety of pharmacological activities[1, 2] such as neurotoxicity, cardiotoxicity, myotoxicity, and hemolytic, anticoagulant and antiplatelet activities.

It has long been observed that the hydrolysis rate catalysed by phospholipase A_2 increases dramatically while the substrates present as multimolecular aggregates and the increase depends on the NaCl concentration. Biochemistry research suggested that NaCl promotes affinity between PLA_2 and the phospholipid interface[3].

Some of PLA_2s from snake venom show hemolytic activity, such as the CMS-9 from *Naja nigricollis* venom[4] and basic PLA_2 from *Agkistrodon halys* Pallas[5]. Studies of the hemolytic mechanism of PLA_2 have been done by chemical modification[6—8]. The first structure of hemolytic PLA_2, the crystal structure of the basic PLA_2 from *Agkistrodon halys* Pallas was determined[9]. According to the structure and the fact that most PLA_2s with hemolytic activity are basic PLA_2s, Zhao *et al.*[10] proposed that a basic residue cluster in C-terminus region might be responsible for the hemolytic activity.

Four kinds of PLA_2 were obtained from the venom of *Dienagkistrodon acutus* through gene engineering[11, 12]. All these PLA_2 were characterized and their amino acid sequences were determined using cDNA method. They were designated as acidic phospholipase A_2I ($aPLA_2$I), acidic phospholipase A_2II ($aPLA_2$II), basic phospholipase A_2 ($bPLA_2$) and Lys^{49}-phospholipase A_2 (Lys^{49}-PLA_2) according to their isoelectric points, which are 4.49, 5.05, 9.49 and 9.3, respectively. It was shown that $aPLA_2$I has an inhibiting effect on platelet aggregation and all phospholipase A_2s except $aPLA_2$II have hemolytic activities. An acidic PLA_2 recently purified from the venom of *Dienagkistrodon acutus* and characterized by Zhang *et al.*[13] displays the same isoelectric point and pharmacological activities as $aPLA_2$I.

This PLA_2 enzyme was crystallized in two crystal

Received: October 22, 2001 Accepted: December 6, 2001
This work was supported by the Chinese Academy of Sciences (No.39970174)

* Corresponding author: Tel, 86-10-64888513; Fax, 86-10-64877837; e-mail, lin@sun5.ibp.ac.cn

forms with the same space group but different unit cell parameters [$P2_1$ (I) and $P2_1$ (II)][13]. In contrast with $P2_1$ (I) form, which was grown in solution containing NaCl, $P2_1$ (II) form was grown in the absence of NaCl. Crystal structure of this enzyme in $P2_1$ (I) has been determined and the relationship between structure and activity of inhibiting platelet aggregation was discussed[14]. In this paper, we report crystal structure determination of $P2_1$ (II) at 0.28 nm resolution and structural comparison with $P2_1$ (I) crystal form, and explore the hemolytic site based on a comparison of the amino acid sequences and the three-dimensional structures.

1 Materials and Methods

1.1 Crystallization and data collection

The PLA_2 enzyme provided for crystalliztion was extracted from the venom of *Dienagkistrodon acutus* (*Agkistrodon acutus*, collected from Jiangxi Province, China) according to the procedure outlined previously[13]. Crystals were grown at 18 °C by the hanging-drop method with 10 g/L of protein, 0.05 mol/L HEPES buffer (pH 7.5) and 35% MPD in 8 μl drops equilibrated against 0.5 ml solution of 0.1 mol/L HEPES buffer (pH 7.5) and 70% MPD. The data were collected with a Mar345 research area detector using a single crystal. The data were scaled and merged using the HKL suite[15]. The crystal belongs to space group $P2_1$ with cell dimensions a = 4.348 nm, b = 7.149 nm, c = 4.385 nm and β = 116.32°. There are two protein molecules in the asymmetric unit according to the Matthews coefficient[16]. The data set contains 5 253 unique reflections with R-merge of 8.4% and completeness of 88.5% (78.6% for the high resolution shell) at 0.28 nm. The details of purification, crystallization and preliminary X-ray analysis of $P2_1$ (II) have been published earlier[13].

1.2 Structure determination and refinement.

The structure was solved by the molecular replacement method using the AMoRe package[17]. The search model used in the cross-rotation function calculation was the dimer from the previously reported $P2_1$ (I) structure (*Dienagkistrodon acutus* $aPLA_2$, 1IJL in the Brookhaven Protein Data Bank). The cross-rotation function search was calculated using the data in the resolution range 0.8—0.4 nm with an integration radius of 1.9 nm. The top 4 peaks of the cross-rotation function were used to calculate the translation functions. The translation function showed that the first peak was the correct solutions judged by their significance of correlation coefficients. The rigid body refinement of Amore resulted in an R factor of 39.8% and a correlation value of 47.7%. The initial model, oriented and positioned according to the molecular replacement solution, was examined on a Silicon Graphics O2 workstation using the program FRODO/TURBO, and the molecular packing in the crystal was confirmed to be reasonable.

The refinement was carried out using the CNS program[18] with 10% of the data reserved to calculate the free R factor[19]. A total of 4 511 reflections in the resolution range 0.8—0.28 nm were used in the refinement. Model building was carried out using the program FRODO/TURBO. The main-chains and side-chains of the molecules were adjusted according to the $2Fo$-Fc and Fo-Fc electron density maps. During the course of the refinement, the R factor was gradually reduced. One calcium ion, one sulfate anion, three MPD (2-methyl-2, 4-pentanediol) molecules and 80 water molecules were included in the model based on the appearance of corresponding electron densities and their environments. After several cycles of atomic position and group B factor refinements and model rebuilding, R value and R-free value were converged, the Fo-Fc map showed no obviously uninterpretable features.

2 Results

2.1 Model quality

The final model gives an R value of 21.9% and an R-free value of 25.7% in the resolution range 0.8—0.28 nm. The $2Fo$-Fc electron density is well defined for both the backbone and the side-chains except for several residues on the molecular surface (Fig. 1). The model has good stereochemistry with *r. m. s.* deviations from ideal values being 0.0012 nm for bond lengths, 2.61° for bond angles and 27.06° for torsion angles. Calculations by the program PROCHECK[20] indicated that most of non-glycine and non-proline residues in the asymmetric unit were located in the most favored regions (163 residues, 81.5%) or the additional allowed regions (33 residues, 16.5%), and only four (2%) in the general allowed regions. The refinement results are listed in Table 1.

2.2 Dimer structure

The sequence of the PLA_2 enzyme has four different residues (Ala^{102}, Ala^{103}, Pro^{131} and Pro^{133}) and one inserted residue (Pro^{122}) in comparison with that of the $aPLA_2I$. The final model consists of all (1 912) non-H protein atoms from two crystallographically independent molecules, one calcium ion, one sulfate anion, three MPD molecules and 80 water molecules. All these atoms occupied 56.8% of the unit cell volume.

Like $P2_1$ (I), the two molecules (A and B) in

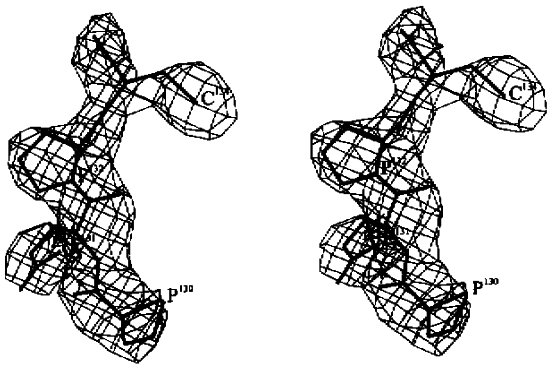

Fig. 1 The fitting of the proline riched C-terminus of molecule A with 2*F*o-*F*c electron density map contoured at the 1.0 σ level

Table 1 The refinement results

R factor (%)	21.90
R-free factor (%)	25.70
Resolution range (nm)	0.8—0.28
Number of reflections	5 039
Model	
Number of non-H protein atoms	1 912
Number of calcium ions	1
Number of water molecules	80
Number of sulfate anion	1
Number of MPD molecules	3
r.m.s. deviations from ideality	
Bond distances (nm)	0.0012
Bond angles (°)	2.61
Dihedral angles (°)	27.06
Improper angles (°)	1.06

the asymmetric unit form a dimer with approximate two-fold symmetry and the dimer is stabillized by large amounts of hydrophobic interactions formed by residues Leu^2, Ile^3, Ile^9, Met^{19}, Phe^{20}, Trp^{21}, Ala^{24}, Trp^{31} and Trp^{119} and five intermolecular hydrogen bonds. The surface area buried by the formation of the dimer is 9.05 nm^2 (program CCP4), corresponding to 14.6% of the monomer surface area, a value close to that of $P2_1$(I) as a typical dimer[21].

The superposition of the dimer in $P2_1$(II) and $P2_1$(I) gives an *r.m.s.* deviation of 0.09 nm for all the Cα atoms. This shows the overall similarity between the two dimers from different crystal forms (Fig.2). If the molecules A from the two forms were superimposed, the two molecules B would deviate with each other only slightly, resulting from minor structural differences in two segments around β-wing and C-terminal ridge, i.e. 76—93, 124—133 for molecule A and 74—90, 124—134 for molecule B (*r.m.s.* deviation > 0.1 nm for the Cα atoms). The comparison between the two crystal forms of the enzyme is important as it indicates the stability of the

Fig.2 Superposition of Cα traces of dimers form different crystal forms, $P2_1$(II) (thick line) and $P2_1$(I) (thin line)

dimer structures.

The two molecules in the asymmetric unit of $P2_1$(II) greatly differ from each other at some local regions, particularly the segment consisting of residues 14—23 (0.825 nm for Cα atom at residue 19), located at the dimer interface. In molecule A, the segment includes a short α-helix (17 to 22), while in molecule B it shows an unusual irregular turn conformation. This observation is consistent with that previously reported for $P2_1$(I)[14]. The different conformation of segment 14—23 seen in $P2_1$(I) is present once again in this new crystal form. Since segment 14—23 involves several residues at the "interface recognizing site" (IRS)[22, 23], that the segment conformation can adapt when it binds to a contacted molecule implies the flexibility of the IRS as suggested previously[14]. This work reinforces this viewpoint. The conformational flexibility of the IRS may be required by the "allosteric activity" of the enzyme-oil/water interface interaction.

2.3 Positively charged residue 34 and hemolytic activity

Dienagkistrodon acutus aPLA$_2$I is the only known member of acidic PLA$_2$s which exhibits hemolytic activity. Careful inspection shows that aPLA$_2$I does not contain as many basic residues at putative hemolytic site as proposed for *Agkistrodon halys* Pallas bPLA$_2$. This implies that not all of the basic residues in the cluster are responsible for the hemolytic activity and only a few residues out of this cluster may be pivotal in exerting the hemolytic activity.

The amino acid sequence comparison of hemolytic group II PLA$_2$ with non-hemolytic group II PLA$_2$ reveals distinct difference at the residue 34 (Table 2). At this position, all of hemolytic group II PLA$_2$ enzymes have a basic residue and all non-hemolytic group II PLA$_2$s have non-basic residues. His^{34} of *Dienagkistrodon acutus* aPLA$_2$ points out of the molecular surface.

The suggestion that the basic residues at position 34 may play a pivotal role in the hemolytic activity was supported by point mutational study of

Table 2 The N-terminus amino acid sequence comparison of the group II PLA_2, showing characteristic differences between hemolytic and non-hemolytic PLA_2

		1 10 20 30 40 50	
Dienagkistrodon acutus	$aPLA_2$	SLIQFETLIM KVVK-KSGMF WYSAYGCYCG WGG GRPQDA TDRCCFVHDC	[11]
Aagkistrodon halys Pallas	$bPLA_2$	H. L. . RKM. K . MTG-. EPVV S. AF. . . . . S. . . . K. K.	[28]
Aagkistrodon halys blomhoffii	$bPLA_2$	H. L. . RDM. K . MTG-. EPVI S. AF. . . . . S. . . . K. KN.	[29]
Dienagkistrodon acutus	$bPLA_2$	. . . . . -. . . . . K. . . . . R. N.	[31]
Dienagkistrodon acutus	K^{49}-PLA_2	. . FELGKM. W QETG-. NPVK N. GL. . . N. . V. . . . E. L. . . . . K.	[11]
Aagkistrodon halys Pallas	$aPLA_2$	. . . . A. -. . . . . N. . . . . Q.	[30]
Aagkistrodon halys blomhoffii	$aPLA_2$	. . M. . . . . IAG-R. . IW Y. GS. . . . . A. . Q. . . . . S.	[31]
Aagkistrodon halys Pallas.	$baPLA_2$	H. L. . RKM. K . MTG-. EPVV S. AF. . . . . S. . Q. K. K.	[27]
Aagkistrodon halys Pallas	$nPLA_2$	N. . . . N. . . . EE. . -. NAIP F. . . . . G. . Q. . . . . G	[32]
Bothrops jararaca	PLA_2	D. W. . GQMMN D. MR-EYVV. N. LY. . . . . I. K. RG.	[33]
Vipera aspis. Zinnikeri	PLA_2	N. F. . AKM. N GKLK-AFSVW N. IS. . . . . Q. T. K.	[34]
Vipera russelli formosensis	PLA_2	N. F. . GEM. L EKTG-. EVVH S. AI. . . . . Q. . A.	[35]

The top five enzymes are all hemolysins, and the remaining are non-hemolytic. It is very clear that all of the PLA_2s with hemolytic activity possess a basic residue at 34 position. The blanks in the sequences are based on a homology numbering scheme in the large family of PLA_2 molecules, derived from the bovine pancreatic PLA_2 sequence[24—26].

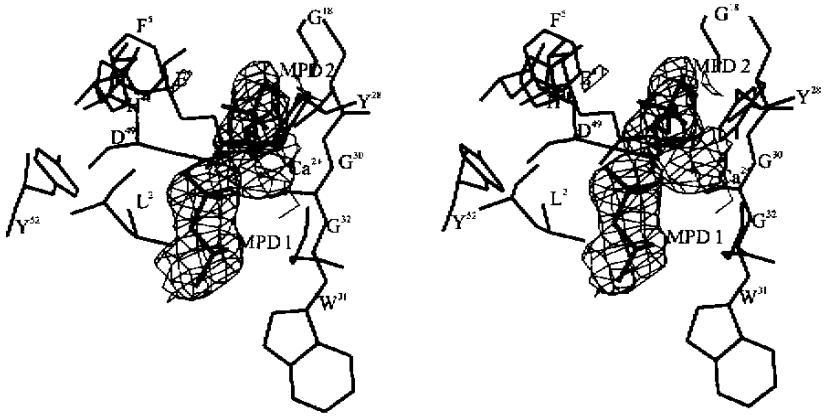

Fig.3 Two MPD molecules (MPD 1 and MPD 2) located at the bottom of the hydrophobic channel (molecule A)
MPD 1 is coordinated by the calcium ion.

Agkistrodon halys Pallas $bPLA_2$, in which when the positively charged Arg^{34} was changed to a negatively charged residue or a neutral residue, the hemolytic activity was significantly decreased (see accompanying paper[36]).

2.4 Ca^{2+} ions and MPD molecules

Calcium is an essential cofactor for the catalytic activity of phospholipase A_2. In the present structure, calcium ion is missing in the molecule B, but evidently occupies the expected position around the calcium binding loop of molecule A, although we did not add Ca^{2+} to the crystallization solution. A structural comparison of the calcium binding loops for both molecules shows no remarkable difference in their overall conformation. This implies that the presence of a calcium ion does not influence the loop structure significantly.

Deinagkistrodon acutus $aPLA_2$ was crystallized in $P2_1$ (II) from MPD with high concentration (35%). Three MPD molecules are visible in the structure. Two MPD molecules (MPD 1 and MPD 2) are located at the bottom of the hydrophobic channel leading to the active site of molecule A. The other one is positioned at the hydrophobic channel of molecule B. The MPD molecules bind in the hydrophobic channel mainly through hydrophobic contacts. Hydrogen bonds to the protein molecules also contribute to these interactions. One MPD molecule in molecule A seems to be coordinated by the calcium ion and being more stable than the other two MPD molecules (Fig.3).

2.5 Crystal packing

Both crystal forms of *Deinagkistrodon acutus* $aPLA_2$ belong to $P2_1$ space group, however their unit cell parameters are considerably different. The unit cell parameters of $P2_1$ (II) (a = 4.348 nm, b = 7.149 nm, c = 4.385 nm and β = 116.32°) are in contrast with those of $P2_1$ (I) (a = 4.871 nm, b = 3.800 nm, c = 6.990 nm and β = 99.35°). In the two crystal forms, the dimer structures are similar,

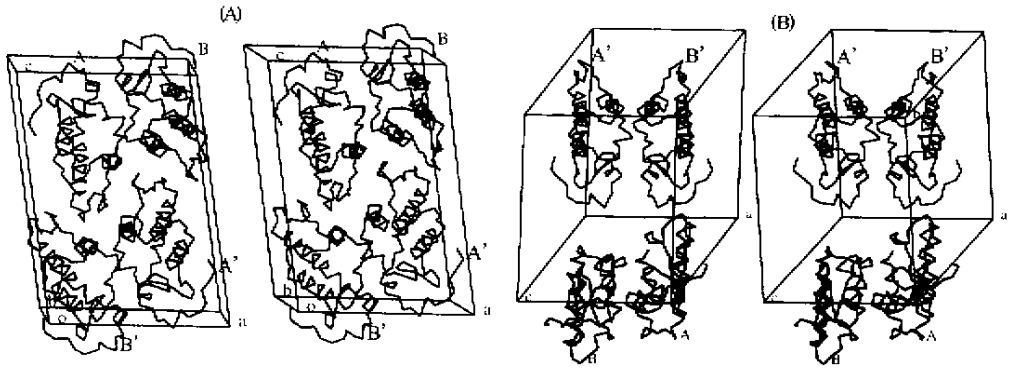

Fig.4 Comparison of the two dimer packing

(A) $P2_1$(I), the non-crystallographic two-fold axes of the dimers run parallel to each other. (B) $P2_1$(II), the non-crystallographic two-fold axes of the two dimers are approximately perpendicular to each other.

whereas the patterns of the dimer packing differ greatly.

Fig.4 represents dimer packing of the two crystal forms. In the unit cell of $P2_1$(I), the two dimers extend along the *c* axis and the two non-crystallographic two-fold axes of the two dimers run parallel with each other and deviates 13.1° from *c* axis. While in $P2_1$(II) the two dimers extend along the *b* axis, the two-fold axes of the two dimer are approximately perpendicular to each other and one of them deviates 14.4° from *b* axis.

In $P2_1$(I) form, one Zn^{2+} ion was found to connect two His^{34} residues from two adjacent dimers, while in $P2_1$(II) form, such metal-mediated interactions are absent.

The different crystal packing leads to different dimer-dimer contact regions in the two crystal forms. In $P2_1$(I), the dimers contact with each other tightly through jagged interlock. The molecule A in a dimer only forms tight interactions (hydrogen bonds and hydrophobic interactions) with molecule B in a neighboring dimer and *vice versa*. The contact regions mainly involve segments 86—91, 113—126, 131—134 of molecule A and 1—5, 114—132 of molecule B. In $P2_1$(II), molecule A forms extensive interactions only with molecule B from adjacent dimers; however, molecule B has extensive interactions with both molecules B and A from adjacent dimers. The contact regions here mainly involve segments 30—43, 71—85, 111—118 of molecule A and 85—92, 130—134 of molecule B.

3 Discussion

It has long been observed that the increased hydrolysis rate of phospholipase A_2 on substrates presenting as multimolecular aggregates depends on NaCl concentration. The interfacial rate enhancement was attributed to three factors: (a) promotion of PLA_2 binding by net anionic charge of the interface; (b) enhancement of substrate affinity of PLA_2 at the interface; and (c) stimulation of the rate-limiting chemical step[3]. The structural analysis and comparison of the two crystal forms of *Deinagkistrodon acutus* $aPLA_2$ correlate with this viewpoint.

The differences between the structures of $P2_1$(I) and $P2_1$(II) can be summarized into three main points: calcium ion's occupancy in the calcium binding loop, the presence or absence of MPD molecules in the hydrophobic channel and the pattern of dimer's packing. These differences may reflect the effect of the presence of NaCl as well as the concentration of MPD.

This work shows the stability of the dimer of *Deinagkistrodon acutus* $aPLA_2$ in different crystallization conditions and the dependence of the dimer packing on the crystallization conditions. Careful examination indicates that the intra-dimer interactions of *Deinagkistrodon acutus* $aPLA_2$ mainly consist of hydrophobic interactions, whereas the inter-dimer interactions mainly involve hydrophilic interactions (hydrogen bonds). It implies that the presence of NaCl or the change of ionic strength has significant influence on the hydrophilic interactions between dimers, resulting in different crystal forms.

In $P2_1$(I) form both molecules in the asymmetric unit bind calcium ions, but in $P2_1$(II) form only the molecule A binds a calcium ion. This suggests that NaCl may improve affinity of PLA_2 to its cofactor. The molecule A has high catalytic activity during interfacial catalysis. The molecule B with unusual conformation for segment 14—23, however has low catalytic activity. The molecule B may bind the calcium ion only in the presence of NaCl.

Unlike $P2_1$(II), there is no MPD molecule in the $P2_1$(I) structure. The MPD molecules locate at the hydrophobic channel and might mimic the fatty acid chains of a substrate analogue bound in the active

site. The presence of MPD in the hydrophobic channel in one form but not in the other indicates that NaCl may affect the charge's environment of the hydrophobic channel and then affect the affinity of PLA_2 to its substrate.

The influence of NaCl on the interactions between PLA_2 molecules implies that the ion strength will affect the distribution of charges on the protein surface, and thus affect the interactions between the enzyme and the oil-water interface.

Acknowledgements We thank Dr. ZHAO Xu-Dong for his help during data collection and processing.

References

1 Gowda VT, Schmidt J, Middlebrook JL. Primary sequence determination of the most basic myonecrotic phospholipase A_2 from the venom of *Vipera russelli*. *Toxicon*, 1994, **32**: 665—673

2 Betzel C, Genov N, Rajashankar KR, Singh T P. Modulation of phospholipase A_2 activity generated by molecular evolution. *Cell Mol Life Sci*, 1999, **56**: 384—397

3 Berg OG, Rogers J, Yu BZ, Yao J, Romsted LS, Jain MK. Thermodynamic and kinetic basis of interfacial activation: Resolution of binding and allosteric effects on pancreatic phospholipase A_2 at zwitterionic interfaces. *Biochemistry*, 1997, **36**(47): 14512—14530

4 Lee CY, Hod CL, Eaker D. Cardiotoxin-like action of a basic phospholipase A isolated from *Naja nigricollis* venom. *Toxicon*, 1977, **15**: 355—356

5 Wu XF, Jiang ZP, Chen Y C. A comparison of three phospholipase from the venom of *Agkistrodon halys* Pallas. *Acta Biochim Biophys Sin*, 1984, **16**: 664—671
(引自:生物化学与生物物理学报)

6 Yang CC, King K. Chemical modification of the histidine residue in basic phospholipase A_2 from the venom of *Naja nigricollis*. *Biochim Biophys Acta*, 1980, **614**: 373—388

7 Yang CC, King K, Sun TP. Chemical modification of lysine and histidine residues in phospholipase A_2 from the venom of *Naja naja atra* (Taiwan cobra). *Toxicon*, 1981, **19**: 645—659

8 Condrea E, Fletcher JE, Rapuano BE, Yang CC, Rosenberg P. Dissociation of enzymatic activity from lethality and pharmacological properties by carbamylation of lysines in *Naja nigricollis* and *Naja naja atra* snake venom phospholipases A_2. *Toxicon*, 1981, **19**: 705—720

9 Zhao KH, Song SY, Lin ZJ, Zhou YC. Structure of a basic phospholipase A_2 from *Agkistrodon halys* Pallas at 2.13 Å resolution. *Acta Cryst D Biol Crystallogr*, 1998, **54**: 510—521

10 Zhao KH, Zhou YC, Lin ZJ. Structure of basic phospholipase A_2 from *Agkistrodon halys* Pallas: Implications for its association, hemolytic and anticoagulant activities. *Toxicon*, 2000, **38**: 901—916

11 Liu XL, Pan H, Yang GZ, Wu XF, Zhou YC. Cloning and sequencing of genes encoding phospholipase A_2 from *Agkistrodon acutus*. *Acta Biochim Biophys Sin*, 1999, **31**(1): 41—45
(引自:生物化学与生物物理学报)

12 Liu XL, Xiong Y, Wu XF, Zhou YC. A comparative study of the function of phospholipase A_2 from *agkistrondon acutus*. *Protein and Peptide Letter*, 2000, **7**(2): 83—90

13 Zhang HL, Lin ZJ, Du XY, Zhou YC. Purification, crystal growth and preliminary X-ray analysis of a phospholipase A_2 from venom of *Agkistrodon acutus*. *Acta Biochim Biophys Sin*, 2000, **32**(4): 337—341
(引自:生物化学与生物物理学报)

14 Gu LC, Zhang HL, Song SY, Zhou YC, Lin ZJ. Crystal structure of an acidic phospholipase A_2 from the venom of *Deinagkistrodon acutus*. *Acta Cryst D Biol Crystallogr*, 2002, **58**(1): 104—110

15 Otwinowski Z, Minor W. Processing of X-ray diffraction data collected in oscillation mode. *Method Enzymol*, 1997, **276**: 307—326

16 Matthews BW. Solvent content of protein crystals. *J Mol Biol*, 1968, **33**: 491—497

17 Navaza J. Amore: An automated package for molecular replacement. *Acta Cryst A*, 1994, **50**: 157—163

18 Brunger AT, Adams PD, Clore GM, DeLano WL, Gros P, Grosse-Kunstleve RW, Jiang JS *et al*. Crystallography & NMR system: A new software suite for macromolecular structure determination. *Acta Cryst D Biol Crystallogr*, 1998, **54**: 905—921

19 Brunger AT. Free R value: A noval statistical quantity for assessing the accuracy of crystal structures. *Nature*, 1992, **355**: 472—475

20 Laskowski R, Macarthur M, Moss D, Thornton J. Procheck: A program to check stereochemical quality of protein structures. *J Appl Cryst*, 1993, **26**: 283—290.

21 Janin J, Miller S, Chothia C. Surface, subunit interfaces and interior of oligomeric proteins. *J Mol Biol*, 1988, **204**: 155—164

22 Pieterson WA, Vidal JC, Volwerk JJ, De Haas GH. Zymogen-catalyzed hydrolysis of monomeric substrates and the presence of a recognition site for lipid-water interfaces in phospholipase A_2. *Biochemistry*, 1974, **13**: 1455—1460

23 Dijkstra BW, drenth J, Kalk KH. Active site and catalytic mechanism of phospholipase A_2. *Nature*, 1981, **289**: 604—606

24 Dufton MJ, Hider RC. Classification of phospholipases A_2 according to sequence. Evolutionary and pharmacological implications. *Eur J Biochem*, 1983, **137**: 545—551

25 Renetseder R, Brunie S, Dijkstra BW, Drenth J, Sigler PB. A comparison of the crystal structures of phospholipase A_2 from bovine pancreas and *Crotalus atrox* venom. *J Biol Chem*, 1985, **260**: 11627—11634

26 Heinrikson RL. Amino acid sequence of phospholipase A_2-alpha from the venom of *Crotalus adamanteus*. A new classification of phospholipases A_2 based upon structural determinants. *Method Enzymol*, 1991, **197**: 201—14

27 Liu XL, Pan H, Yang GZ, Wu XF, Zhou YC. Cloning, expression and biochemical characterization of a basic-acidic hybrid phospholipase A_2-II from *Agkistrodon halys* Pallas. *Biochim Biophys Acta*, 1999, **1431**: 157—165

28 Pan H, Ouyang L, Yang G, Zhou YC, Wu XF. Cloning of the $BPLA_2$ gene from *Agkistrodon halys* Pallas. *Acta Biochim Biophys Sin*, 1996, **28**: 579—582
(引自:生物化学与生物物理学报)

29 Forst S, Weiss J, Blackburn P, Frangione B, Goni F, Elsbach P. Amino acid sequence of a basic *Agkistrodon halys* blomhoffii phospholipase A_2. Possible role of NH_2-terminal lysines in action on phospholipids of *Escherichia coli*. *Biochemistry*, 1986, **25**: 4309—4314

30 Chen YC, Maraganore JM, Reardon I, Heinrikson RL. Characterization of the structure and function of three phospholipase A_2 from the venom of *Agkistrodon halys* Pallas. *Toxicon*, 1987, **25**: 401—409

31 Tomoo K, Ohishi H, Ishida T, Inoue M, Ikeda K, Aoki Y, Samejima Y. Revised amino acid sequence, crystallization, and preliminary X-ray diffraction analysis of acidic phospholipase A_2 from the venom of *Agkistrodon halys* blomhoffii. *J Biol Chem*, 1989, **264**: 3636—3638

32 Kondo K, Zhang J, Xu K, Kagamiyama H. Amino acid sequence of a presynaptic neurotoxin, agkistrodotoxin, from the venom of *Agkistrodon halys* Pallas. *J Biochem*, 1989, **105**: 196—203

33 Serrano SM, Reichl AP, Mentele R, Auerswald EA, Santoro ML, Sampaio CA, Camargo AC *et al*. A novel phospholipase A_2, BJ-PLA$_2$, from the venom of the snake *Bothrops jararaca*: Purification, primary structure analysis, and its characterization as a platelet-aggregation-inhibiting factor. *Arch Biochem Biophys*, 1999, **367**: 26—32

34 Komori Y, Masuda K, Nikai T, Sugihara H. Complete primary structure of the subunits of heterodimeric phospholipase A_2 from *Vipera a. zinnikeri* venom. *Arch Biochem Biophys*, 1996, **327**: 303—307

35 Wang YM, Lu PJ, Ho CL, Tsai IH. Characterization and molecular cloning of neurotoxic phospholipases A_2 from Taiwan viper (*Vipera russelli formosensis*). *Eur J Biochem*, 1992, **209**: 635—641

36 Jiao HM, Jin Q, Zhao JJ, Feng B, Wu XF, Zhou YC. The hemolytic site of the basic phospholipase A_2 from *Agkistrodon halys* Pallas. *Acta Biochim Biophys Sin*, 2002, **34**(3): 383—387

(引自:生物化学与生物物理学报)

尖吻蝮蛇毒酸性磷脂酶 A_2 的新晶型结构

谷立川 张海龙 宋时英 周元聪[1] 林政炯 *

(中国科学院生物物理研究所生物大分子国家重点实验室,北京 100101;[1] 中国科学院生物化学与细胞生物学研究所,上海 200031)

摘要 从尖吻蝮蛇毒中分离出一种酸性磷脂酶 A_2,得到了一种新的晶型。用分子置换法测定其晶体结构,结构的分辨率达到 0.28 nm。该结构给出 21.9% 的晶体学 R 因子(R-free = 25.7%)和合理的立体化学参数。与已报道的晶型相似,不对称单元的两个独立分子形成二体,揭示了这种二体的稳定性。二体的形成过程也伴随着 14 ~ 23 肽段显著的构象变化,这一肽段属于磷脂酶 A_2 的界面识别部位。氨基酸序列分析表明,带正电荷的 34 位残基是所有第二类具有溶血活性磷脂酶 A_2 的共同特点。NaCl 对晶体的堆积具有显著的影响,从而导致晶胞参数的明显改变。与已报道的晶型不同,在酶分子的疏水通道内观测到了 2-甲基-2,4 戊二醇(2-methyl-2,4-pentanediol, MPD)分子。

关键词 磷脂酶 A_2;X 射线晶体学;三维结构;溶血活性;界面催化

收稿日期:2001-10-22 **接受日期**:2001-12-06

中国科学院科学基金资助(No.39970174)

* **联系人**:Tel, 010-64888513;Fax, 010-64877837;e-mail, lin@sun5.ibp.ac.cn